

Co-channel Interference Assessment for Line-of-Sight and Nearly Line-of-Sight Millimeter-Waves Cellular LMDS Architecture

Shayan Farahvash and Mohsen Kavehrad,¹ FIEEE

Behavior of co-channel interference in fixed wireless cellular systems, such as millimeter-waves Local Multipoint Distribution Service (LMDS), is different compared to what has been established for mobile microwave systems. This is due to utilization of a high-gain antenna for the subscriber. In this paper, first the analysis of signal-to-interference ratio (*SIR*) is presented for line-of-sight and nearly line-of-sight LMDS architecture. In this analysis, the effects of precipitation and foliage attenuation and depolarization have been considered. These two parameters have negligible effect on the microwave mobile systems but in millimeter-wave range are among the most important factors in the link budget. To mitigate the fading due to shadowing by buildings and trees, a highly overlapped architecture and macro-diversity are proposed. After analysis of downlink *SIR* in previously proposed cellular systems, a cellular architecture is proposed based on polarization interleaving and frequency segmentation which has a much higher *SIR* yield. The statistical assessment of *SIR* is accomplished by assuming lognormal distribution for the received signals.

INTRODUCTION

It has long been known that a major bottleneck in delivering multimedia services to the telephony subscribers is the low capacity local loop. With ever-increasing demand for higher capacities, the need for broadband local loop access is transformed from a convenience to a necessity. Providing service in such a broadband access loop using a wireless approach has the advantages of network being rapidly deployable and cost-effective. In fact, the cost-effectiveness of the wireless broadband local loop was the most important driving force behind the promotion of such systems. The economic advantages and speed of deployment of the PCS and cellular phone systems encourage an extension of

the same technology to broadband wireless local loop. Originally, pursuing this concept did not get much attention due to the unavailability of enough radio bandwidth to deliver wideband services and the fact that the lower microwave frequencies were already overcrowded. Recently, FCC auctioned more than 1 GHz of bandwidth in the millimeter-wave region for the deployment of a so-called local multipoint distribution service (LMDS). This unprecedented huge available spectrum is another incentive to consider the wireless technology in general, and the LMDS, specifically, as an attractive way of realizing a broadband local loop.

The wireless channel in millimeter waves is a very harsh transmission medium. A signal transmitted in millimeter wave frequencies is subject to severe attenuation by rain and foliage and a high degree of depolarization [1–6]. To overcome this attenuation and have an acceptable fade margin, the utilization of high-gain antennas in an LMDS link seems inevitable. Such a high-

¹Center for Information and Communications Technology Research (CICTR), Department of Electrical Engineering, The Pennsylvania State University, University Park, PA 16802. E-mail: mkavehrad@psu.edu

gain antenna drastically reduces the multipath-induced delay spread to values well below 10 ns [3]. In addition, such an antenna in millimeter-wave frequencies is much smaller than its counterpart in the microwave frequencies and therefore can be conformed at subscriber premises, easily. Incorporating these antennas in LMDS links, however, makes the link highly susceptible to shadowing by buildings or trees [6]. If the direct path between the base station and the subscriber antenna is obstructed by an object which covers the first Fresnel zone, the receiver can not gather a descent signal for further processing.

In cellular wireless networks, it has long been known that the limiting factor for the system performance is co-channel interference [7]. It is safe to say that LMDS, with a high frequency reuse, is no exception to this rule. However, the behavior of signal-to-interference ratio (*SIR*) in cellular LMDS is very much different from what has been understood for traditional mobile systems operating at lower microwave frequencies, due to the following reasons. First, the presence of a high-gain antenna makes the influence of some of the interfering sources more pronounced than others, i.e., those sources in the direction of the antenna's main beam have more disturbing effect than the ones behind it. Second, no clustering concept seems to be feasible in LMDS mainly due to the fact that the demand on the bandwidth for the local loops is so high that the available bandwidth can not be used partially in each cell. Hence, by default, in each cell, all the available bandwidth must be used at least once [8, 9].

The subject of co-channel interference evaluation and its relation to frequency reuse factor, cell shape, diversity scheme, has been an active research area since early 80's [7], [10–15]. Calculation methodology for average signal to average interference ratio (\bar{S}/\bar{I}) in cellular architectures is based on the assumption that the large-scale variation of the signal can be represented by a lognormal distribution and its average value obeys a power law model. To address the statistical behavior of *SIR*, Cox [7] evaluated the sum of identically distributed interference power levels by means of a Monte-Carlo study and computed an outage probability for a mobile located in the corner of either a hexagonal or a square cell. Yeh and Schwartz developed an analytical approach to calculate the cumulative distribution function of the sum of lognormally distributed interference signals and then used the results to evaluate the cumulative distribution function (CDF) or *SIR* [10]. Later, they showed that actually a three-branch macro-diver-

sity scheme can achieve 11 dB improvement in *SIR* over the case of centrally-located base stations with omnidirectional antennas [11]. In another important observation they found the mobile-to-base and the base-to-mobile *SIR* statistics to be almost identical in all cases they studied. Although, there is a general agreement that the Schwartz-Yeh method provides a fairly accurate estimate for the moments of total interference, but in recent years, there has been some arguments on the accuracy of this method in predicting the CDF of *SIR* and it was shown that some simpler methods offer a better accuracy under certain conditions [12].

Assessment of the co-channel interference in fixed cellular systems generally, and for LMDS specifically, considering the effect of both rain fading and foliage depolarization, is the subject of this paper. It should be noted that our case study is for line-of-sight (LOS) or nearly line-of-sight situations where the foliage is the main reason for shadowing. Because our simulations involve finding both outage and \bar{S}/\bar{I} , we choose the Shwartz-Yeh method to find the moments of sums of lognormal random variables.

The organization of the paper is as follows. In Section II, we propose a highly-overlapped cellular architecture for mitigating the shadowing using the well-known concept of macro-diversity. Section III is devoted to calculation procedures for the co-channel interference in LMDS. Here, we will outline some of the specific relations for finding the rain attenuation and cross-polarization-discrimination (*XPD*) in millimeter-waves. Based on this formulation *CDF(SIR)* and \bar{S}/\bar{I} for several different cellular LMDS architectures are analyzed and presented in Section IV and V. Also, we will propose a methodology for designing cellular systems with higher *SIR values*, using polarization interleaving and frequency segmentation.

I. LMDS CELLULAR ARCHITECTURE

In this section, we propose a cellular architecture for an area which is supposed to be covered by an LMDS infrastructure via the well-known concepts of cellular designs and frequency reuse. A complete coverage of an area is possible by different cell shapes. To convey the basic concepts, we assume the cell shape to be square with four base stations at the corners of each cell. The other cell shapes and different strategies of base station placement have been investigated earlier ([13, 14]) and

our work can be extended to these structures, easily. Furthermore, results of [7] show that, in general, difference between the performance of the two systems with two different cell shapes are smaller than the difference due to the uncertainty in other system parameters. Each base station is assumed to be equipped with four 90° sector antennas. It has been shown that square shape cells with four antennas in the four corners have the best relative coverage factor among all other cellular shapes [14].

The existence of a highly directional antenna (more than 30 dBi gain) makes an LMDS link highly vulnerable to shadowing. A well-known countermeasure for shadowing is macro-diversity where any receiver has the ability to access multiple transmitters. For LMDS, we consider a highly-overlapped cellular architecture and a maximum selection combining approach. This situation is shown pictorially in Figure 1(a). In Figure 1(b), the same situation is shown in a more schematic way.

Such a simple macro-diversity scheme can significantly increase the chance of having an acceptable desired signal level. To find improvements gained by

macro-diversity, first a channel model must be established. Lognormal statistics have been the dominant choice for modeling the shadowing in widely different propagation media. It has been shown that a lognormal distribution represents the measured data better than Rician, albeit there could be a near-LOS path between the transmitter and the receiver [3, 18]. In macro-diversity, a subscriber will measure the power from each base station and selects the one with the highest power available (maximum selection diversity). Considering a lognormal distribution, one can find the improvement in the average received signal power for an L -branch maximum selection combining system. The cumulative probability distribution function (CDF) of the desired signal is simply the multiplication of CDF values of the received signal from each base station [19]. For the worst case point in the center of the cell, where the signals from all base stations have the same average power, this will be the CDF of one signal raised to a power L . In this case, CDF of the received signal can be obtained from

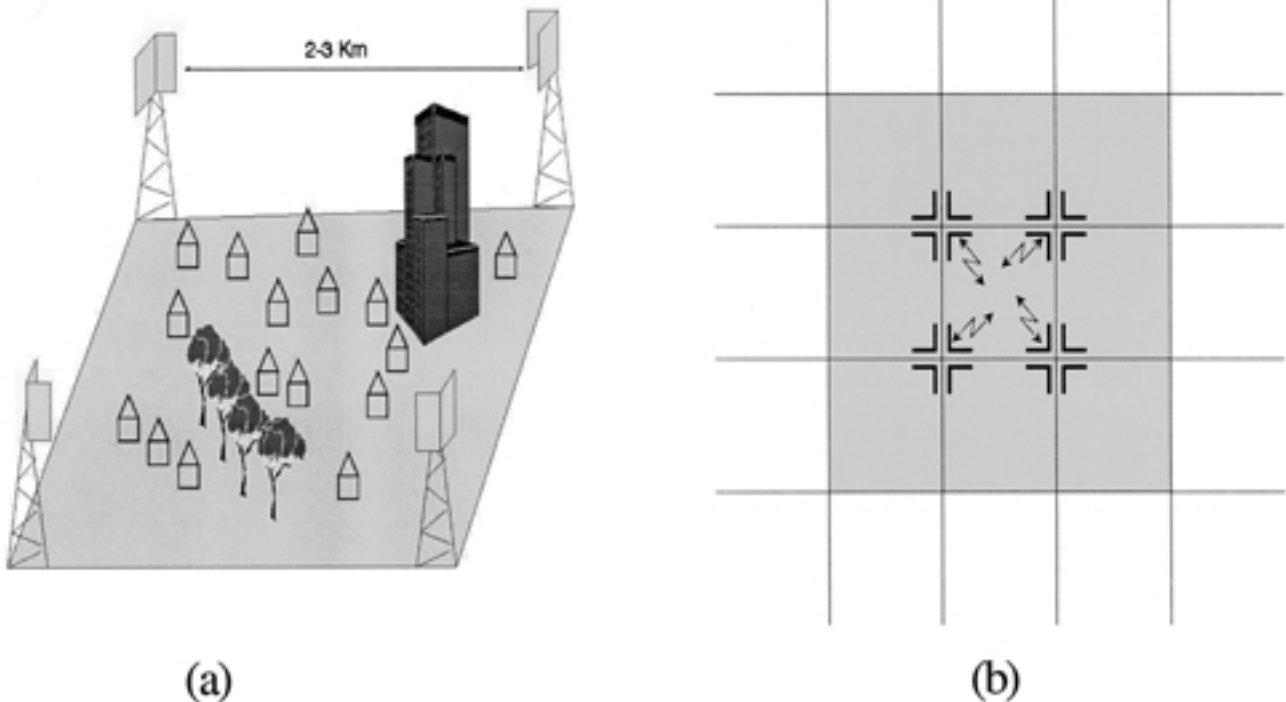


Fig. 1. (a) Four branch diversity using 90° sector antennas to overcome the shadowing by buildings and trees. (b) The schematic picture of macro-diversity. Each subscriber has the opportunity to choose one of the four corner base stations.

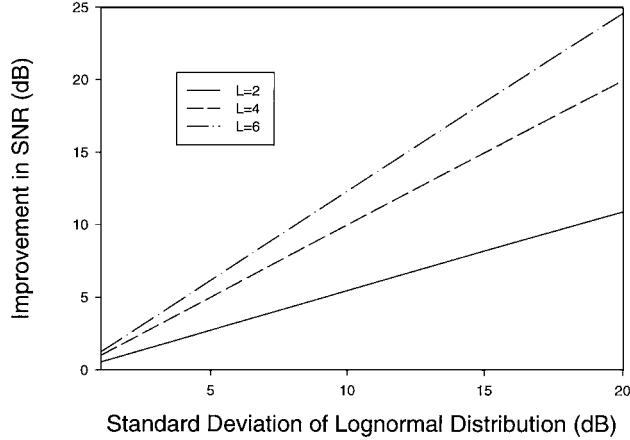


Fig. 2. Improvement in the desired signal power using maximum selection macro-diversity for lognormally distributed signals and for $F_S(s) = 0.5$. L : number of diversity channels.

$$F_S(s) = \prod_{i=1}^L F_{S_i}(s_i) = \left[\frac{1}{2} + \frac{1}{2} \operatorname{Erf} \left(\frac{s - S_1}{\sigma\sqrt{2}} \right) \right]^L \quad (1)$$

where S_1 is the average value of signal power in one of the branches and σ is the dB standard deviation of the lognormal channel model. Figure 2 shows the SNR improvements in comparison with the case when there is no diversity ($L = 1$) as a function of the standard deviation of lognormal distribution and for a fixed probability of signal reception. Improvement in signal power due to macro diversity for a certain value of $F_S(s)$ can be assessed using

$$\Delta s = \sqrt{2}\sigma_s [\operatorname{Erf}^{-1}(2 \sqrt[L]{F_S(s)} - 1) - \operatorname{Erf}^{-1}(2F_S(s) - 1)]. \quad (2)$$

The standard deviation of the received signal is a major factor in determining the amount of improvement. In microwave wireless systems, a typical value of standard deviation is between 8 dB to 12 dB [17], which for a four branch diversity promises 10 dB improvement in the SNR . For millimeter waves propagation, this value is not very well known. However, it can be inferred that due to the vulnerability of these signals to any kind of shadowing, the standard deviation for millimeter waves should be larger and therefore the macro-diversity is more suitable in increasing the available SNR .

By nature, a highly-overlapped structure suffers from co-channel interference, specially if the entire available bandwidth is to be used by all corner base station antennas. In fact, due to the high capacity expected of LMDS, it is assumed the entire bandwidth should be made available to the cell subscribers. That is, in each cell, we have to have a frequency reuse of at least 1. Frequency reuse is defined as the number of times the available bandwidth is used within a particular cell. This is in direct contrast with lower microwave frequency services where only part of the available spectrum is used in each cell and by using the clustering concept, the interference level in the whole structure is minimized. It can be argued that migrating from micro-cellular to a pico-cellular architecture can relax this condition. However, due to the relative cost-effectiveness, micro-cellular architectures are claimed to be optimum [8, 9]. Hence, micro cellular systems are the preferred choice in this paper.

II. CO-CHANNEL INTERFERENCE CALCULATION OVERVIEW

The reuse of radio frequencies makes co-channel interference a fundamental consideration in micro-cellular radio systems. In fact, for almost all cellular systems, a limiting factor in the performance is the co-channel interference and not noise. It is universally accepted that the SIR is a good measure by which one could evaluate the level of interference in a cellular radio system. Since both the desired signal and interference vary randomly, a more meaningful performance measure is the expected probability that the SIR is below an acceptable level (outage probability). The objective of this section is to provide an overview on calculation procedure for obtaining \bar{S}/\bar{I} and outage. The existence of high-gain antenna and rain fading are two important parameters that make the LMDS distinct from its lower frequency counterparts and therefore they should be integrated in this procedure. Also, considering that there are many system proposals for LMDS which use both horizontal (H) and vertical (V) polarizations, it is imperative to incorporate the depolarization into these calculations.

A. Desired Signal and Interference Power

Except for a constant factor, the average desired signal from a base station can be obtained according to a well-known radio link formula:

$$S_1 = 10 \log_{10} \left(\frac{P_t G_b G_s L_{rain}}{r^m} \frac{XPD - 1}{XPD} \right) \quad (3)$$

where P_t is the transmitted power and G_b and G_s are the gain of base station and subscriber antennas respectively, m is the attenuation exponent in power law model, XPD (Cross-polarization discrimination) is a quantitative measure for depolarization and L_{rain} is the attenuation by rain. Modeling the wave propagation in an urban environment has been the subject of many research papers [1–6]. Reports on the typical values for m in power law model, however, are rare. Recently, it has been shown that m is a strong function of vegetation density in the area and the base station antenna height [3]. Specially, the antenna height can drastically reduce the value of m . This is mainly due to the fact that at higher antenna levels, the probability of blockage by trees will be reduced and therefore the millimeter-wave signal will experience less attenuation. In our calculations, we consider m to have values between 4 to 6, representing an area with low to moderate density of foliage [3, 9].

The effect of rain attenuation in millimeter-wave communication systems is an active research area [11]. For our purpose, we use the following heuristic formula which has wide acceptance [8]

$$L_{rain} = -aR^b \text{ (dB/Km)}. \quad (4)$$

In equation (4), R is the rain rate in mm/hr and constants a and b are different for different polarizations:

$$a_h = 0.187, \quad b_h = 1.021 \quad (5.a)$$

$$a_v = 0.167, \quad b_v = 1.0 \quad (5.b)$$

It can be seen that the difference between the rain attenuation of different polarizations is insignificant, e.g., for a rain rate of 10 mm/hr the difference is only 0.3 dB/Km. Therefore, to simplify our calculation, we only use the horizontal polarization values to calculate the rain attenuation.

For rain, XPD can be found via the semi-empirical relationship provided by CCIR [4]. Another main source of depolarization is vegetation. In fact, experimental results show that the depolarization by trees is an order of magnitude larger than the corresponding values for rain depolarization [3]. Figure 4 shows the comparison between XPD due to rain and vegetation. As it can be seen, vegetation depolarization is the dominant fac-

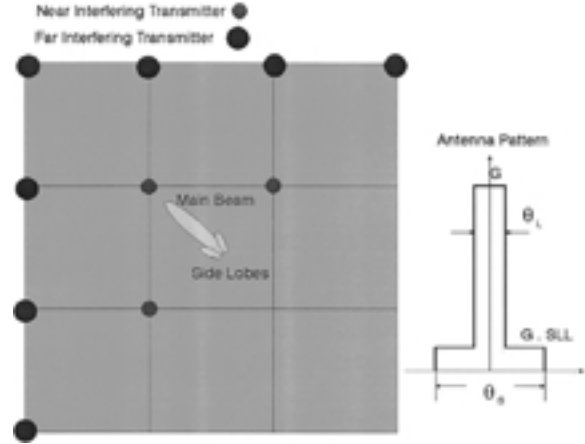


Fig. 3. Interference sources and simplified antenna pattern in a cellular architecture for LMDS. The subscriber is assumed to be at the center of central cell equipped with a high-gain antenna. Cell shape is square and only the first tier of surrounding cells is shown.

tor and therefore in our calculations we neglect the rain effect, compensated for by the higher gain of the antennas used, in nearly line-of-sight cases. Furthermore, XPD is a very weak function of co-polarized attenuation and therefore as another simplifying assumption, we consider a constant value of $XPD = 16$ dB for our calculations. In fact, Figure 8 of reference [3] clearly shows that most of the measured data values are actually around a XPD value of 16 dB.

The average received power from j -th interference source can be written as

$$\left\{ \begin{array}{l} \bar{I}_j = 10 \log_{10} \left(\frac{P_t D_b D_s L_{rain}}{r^m} \frac{1}{XPD} \right) \\ \quad \text{for a cross-polarized source} \\ \bar{I}_j = 10 \log_{10} \left(\frac{P_t D_b D_s L_{rain}}{r^m} \frac{XPD - 1}{XPD} \right) \\ \quad \text{for a co-polarized source} \end{array} \right. \quad (6)$$

where D_b is the directivity of the interfering base station antenna in the direction of subscriber and D_s is the directivity of the subscriber in the direction of the interfering base station. A simplified radiation pattern of the antenna is shown in Figure 3, where antenna has only two side lobes with constant side lobe level of SLL (dB). Following this simplifying assumption on the shape of the radiation pattern of antenna, D can be either G or $G.SLL$ or zero;

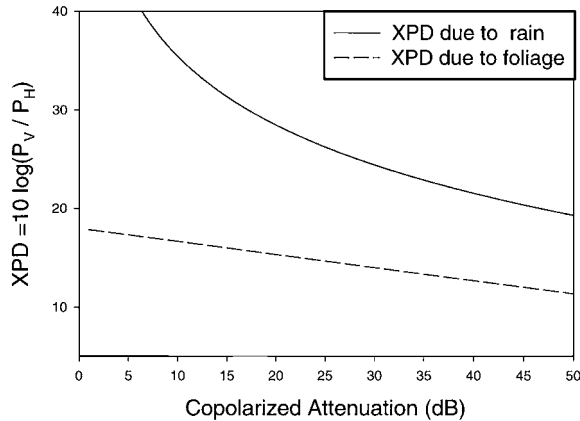


Fig. 4. XPD for rain and foliage. Rain depolarization is found for zero tilt and elevation angles [4]. Foliage depolarization is shown as a linear fit to the measured data [3].

$$D = \begin{cases} G & |\theta| \leq \theta_L/2 \\ 0 & |\theta| \geq \theta_S/2 \\ G.SLL & \text{Otherwise} \end{cases} \quad (7)$$

The values of G , SLL , θ_S , θ_L for base station antenna and for subscriber antenna are shown in Table 1. θ_L is roughly the beamwidth of the antenna and θ_S is the angular span of the non-zero values for the antenna pattern. Pattern of an antenna in real world can have a very complex shape and equation (7) is an abstract expression for it. It should be noted that our case study is for line-of-sight (LOS) or nearly line-of-sight situations where the foliage is the main reason for shadowing. The experimental results in [3] show that when a tree is obstructing the LOS path, for many cases, it is in the far field region of the antenna. Therefore using free-space values of G and SLL seems to be reasonable. Finally, using equation (7) has this implicit assumption that all the non-line-of-sight interfering base stations are equally important. This renders our simulation to be a worst case analysis which is in harmony with the rest of this paper, as we shall see.

B. Calculating \bar{S}/\bar{I} and CDF(SIR)

Having set the equations for finding the signal power and the co-channel interference, the next task is to find the main sources of interference. In our analysis of the downlink interference, only the first tier of interfering base stations are considered and effect of farther stations are assumed to be negligible. In addition, the SIR is found at the so-called *worst point* [7] at the center of the cell. Without loss of generality, we assume that the desired base station is at the upper left corner of central cell in Figure 3. Different sources of interference can be partitioned to near and far according to their distance from the *worst point* (Figure 3). Due to the narrow beamwidth of the subscriber antenna and its nearly zero back-to-front ratio, the interference contribution of many sources in the first tier are negligible and contribution of some far co-channel interference sources are actually more than the near ones. The interference contributions from different sources are considered to be independent. For each interfering base station, the average received power can be found using (6). As stated earlier, the statistical behavior of the transmitted signal from any base station can be described by a lognormal random variable with an average value calculated from a power law model. For the total interference power, we need to find a new random variable as the sum of a finite number of lognormally distributed random variables.

$$I = 10 \log_{10} \left(\sum_j 10^{I_j/10} \right) \quad (8)$$

In the literature, there are two different approaches to find statistical behavior of this random variable. In a simplistic approach, considering the fact that the number of interfering transmitters is large and they are independent of each other, central limit theorem is valid and the total interference is assumed Gaussian. Using a more rigorous approach, it has been shown that the sum of two lognormal random variables is best described by another

Table I. Antenna Characteristics for Base Station and Subscriber

	θ_L°	θ_S°	$G(\text{dB})$	$SLL(\text{dB})$
90° Base Station Antenna	90	190	15	-20
Subscriber Antenna	2.4	190	35	-20

lognormal variable. Hence, the sum of finite number of lognormal variables is lognormal, too. To find the statistical parameters (mean and variance) of the sum of finite number of lognormal RV's we used the Schwartz-Yeh method [10]. Despite the recent arguments on the accuracy of this method for estimated *CDF*, it is safe to say that for moments of total interference (including the power) it provides more accurate results and therefore it can be used when such calculations are concerned [12]. In addition, Figure (7) of [12] shows that although outage probability values found by using the simpler Wilkinson's is fairly accurate but Schwartz-Yeh method can provide almost the same accuracy. Considering the total interference to be a lognormal variable, its average and standard deviation (i.e., \bar{I} and σ_I) can be found through an iterative approach described in [10]. It should be mentioned that finding the average and variance of composite lognormal variables using this method is slightly sensitive to the order of combination and some error must be tolerated when using the results. Considering the signal and total interference independent, *CDF* of the dB value of *SIR* can be calculated according to [11]

$$F_{SIR}(sir) = 1 - \int_{-\infty}^{+\infty} f_S(s)F_I(s - sir)ds \quad (9)$$

where the probability density function of signal can be found using equation (1) and the total interference, as mentioned, is lognormal:

$$f_S(s) = L \left[\frac{1}{2} + \frac{1}{2} \operatorname{Erf} \left(\frac{s - S_1}{\sigma\sqrt{2}} \right) \right]^{L-1} \cdot \frac{1}{\sigma\sqrt{2\pi}} \operatorname{Exp} \left[\frac{-(s - S_1)^2}{2\sigma^2} \right] \quad (10)$$

$$F_I(i) = \frac{1}{2} + \frac{1}{2} \operatorname{Erf} \left(\frac{i - \bar{I}}{\sigma_I\sqrt{2}} \right) \quad (11)$$

Also, \bar{S}/\bar{I} can be found easily by subtracting the total interference power from the average value of the desired signal power in a macro diversity scheme;

$$\bar{S}/\bar{I} = \int_{-\infty}^{+\infty} s f_S(s)ds - \bar{I}. \quad (12)$$

As a special case, if we consider the signal and interference values deterministic ($\sigma = 0$), then \bar{S}/\bar{I} can be written in terms of \bar{S}/\bar{I} for each individual interfering source as

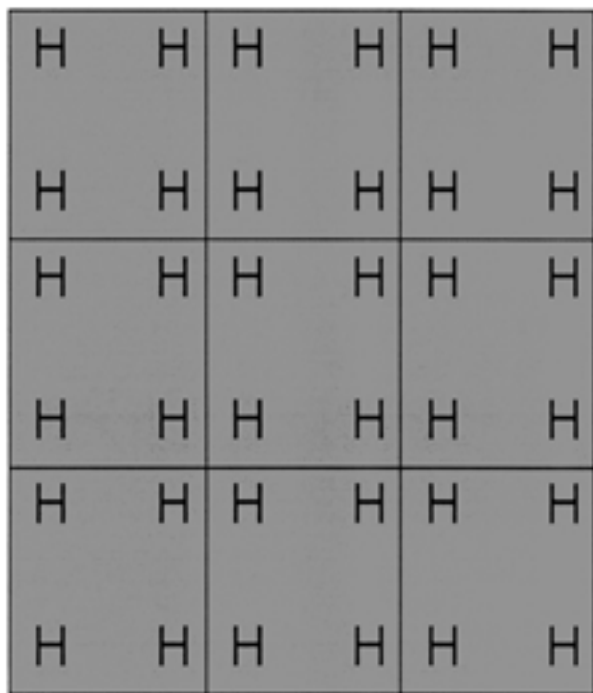
$$\bar{S}/\bar{I} = 10 \log_{10} \frac{10^{\bar{S}/10}}{\sum_j 10^{\bar{I}_j/10}} \quad (13)$$

Using equation (13) has this definitive advantage that the calculation of \bar{S}/\bar{I} will be independent of variance of the received signal which is not very well-known at millimeter-wave frequencies. Later in the paper, it will be demonstrated that using equation (13) provides a lower bound on \bar{S}/\bar{I} , i.e., for any non-zero variance, \bar{S}/\bar{I} will have more than the above value.

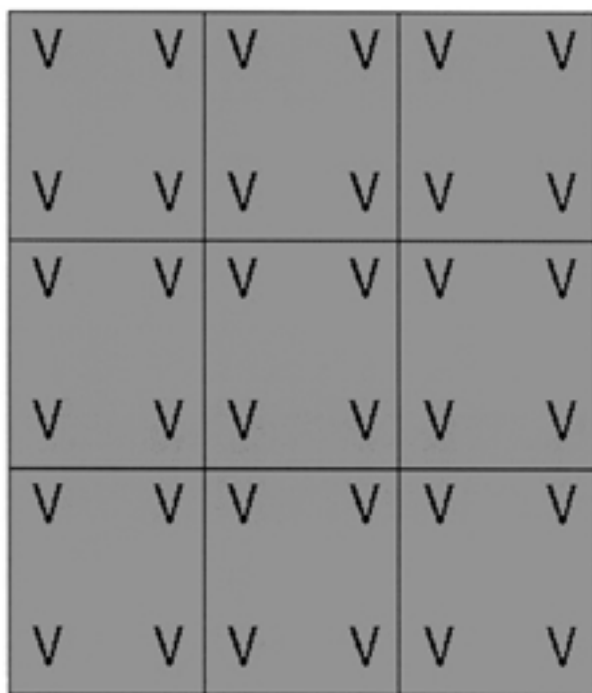
III. \bar{S}/\bar{I} IN LMDS CELLULAR SYSTEMS

Using the formulation developed in the previous section, our intention in this section is to calculate the downlink \bar{S}/\bar{I} for different frequency/polarization assignments to the base stations and to identify the major sources of interference in an LMDS cellular system equipped with a directive antenna for subscribers. Through this analysis, the main interference sources are identified and some guidelines in designing an architecture with maximum \bar{S}/\bar{I} are obtained. The full statistical treatment of the problem is presented in the next section.

\bar{S}/\bar{I} is a strong function of frequency reuse in the system. Due to a high capacity demand on LMDS, here it is assumed that a frequency reuse of 4 is the required minimum, i.e., each corner base station uses the entire available LMDS bandwidth. This assumption prohibits the use of clustering concept in LMDS cellular systems and gives it a distinct feature in comparison with conventional mobile cellular systems. A better use of bandwidth resources is possible by assigning both polarizations and the whole available spectrum to each of the corner base stations, i.e., a frequency reuse of 8. Figure 5 shows two cellular systems with a frequency reuse factor of 4 using a single polarization. To synthesize a cellular system with a frequency reuse of 8, we can overlay these two figures so that each sector antenna is equipped with two transmitters, each using the whole bandwidth on either *H* or *V* polarization. Figure 6 shows the \bar{S}/\bar{I} for $\sigma = 0$ and for two different cellular architectures as a function of attenuation exponent in the power law model



(a)



(b)

Fig. 5. Cellular architectures with single-polarization and frequency reuse of 4. H and V letters at corner of each square-shape cell represent a base station with corresponding polarization using the entire available bandwidth and equipped with a sector antenna.

(*m*). Apparently, for both architectures the level of interference is unacceptably high. It should be remembered that LMDS is proposed to provide a broadband wireless access for data communication and therefore \bar{S}/\bar{I} in this system should be much higher than the conventional mobile cellular architectures for voice transmission. To have a base for comparison, from now on we call the cellular architectures in Figure 5 the reference architecture.

Investigating the contribution of different sources to the total interference, it can be seen that the main sources of interference are the near interferers, i.e., those that are in one of the corners of the relevant cell. Between all the far interferers, the one that is in the adjacent cell directly in front of the subscriber's antenna main beam is the most problematic one. This source becomes less important as the medium becomes more attenuative. Due to a subscriber's highly-directive antenna, the effect of other far interferers are very small. Based on these observations, other cellular architectures are proposed whereby

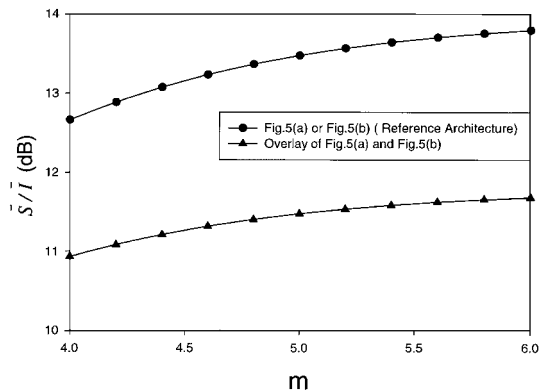


Fig. 6. \bar{S}/\bar{I} for the reference architectures of Figure 5 (frequency reuse of 4) and for their overlay to form a system with frequency reuse of 8 by using both polarizations. Horizontal axis is the exponent in power law model. ($\sigma = 0$)

using the intracell and intercell polarization interleaving, co-channel interference is reduced. Figure 7 shows sam-

ples of such architecture with a frequency reuse of 4 and Figure 8 shows \bar{S}/\bar{I} ($\sigma = 0$) along with \bar{S}/\bar{I} from the reference architecture. As it can be seen, performance improvement of several dBs is possible.

For increasing the \bar{S}/\bar{I} to a higher value, bandwidth segmentation and polarization interleaving must be incorporated in a cellular architecture, simultaneously. For this purpose, the available bandwidth can be divided into four different segments. For systems with a frequency reuse factor of 1, each bandwidth segment can be assigned to one of the corner base stations and to avoid interference from the far interferers, the corresponding base station can be assigned to a different bandwidth segment. Four of such architectures are shown in Figure 9, where no polarization interleaving was applied to

them, individually. To obtain a cellular architecture with a higher frequency reuse, the architectures in Figure 9 can be overlaid. For instance, a frequency reuse of 2 can be obtained by overlaying Figure 9(a) and (b) and frequency reuse of 4 can be implemented by overlaying all the configurations in Figure 9. To obtain the latter with a higher \bar{S}/\bar{I} , we use the following general design guidelines. For any corner base station, the available bandwidth is used only once and adjacent bands are transmitted on different polarizations. Also, with respect to the desired base station in the center cell, the near and far sources of interference should not be in the same frequency band or at least they should be on different polarizations.

Figure 10 clearly shows that following the previ-

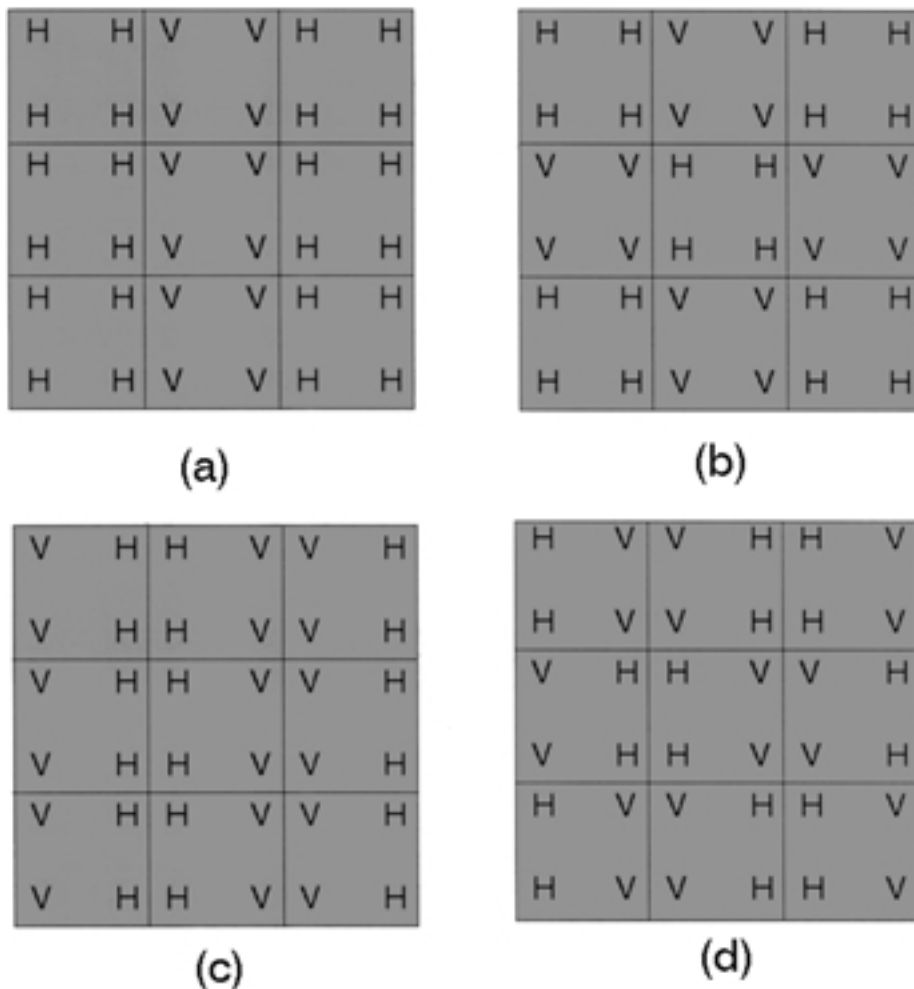


Fig. 7. Four samples of cellular architectures with frequency reuse of 4 and polarization interleaving.

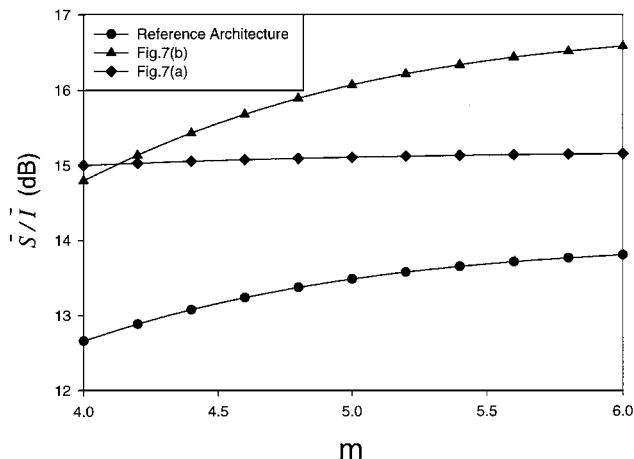


Fig. 8. Similar to Figure 6 but for two samples of cellular architecture in Figure 7.

ous guidelines can significantly increase the \bar{S}/\bar{I} . A close inspection of Figure 10 reveals that the proposed architecture promises 5 to 10 dB improvement in the \bar{S}/\bar{I} for the range of desired m 's when compared with the reference architecture where no polarization interleaving or bandwidth segmentation is used. As it can be seen from Figure 8, in a similar situation, the previously proposed configurations with a simple polarization interleaving promise only 2 dB to 3 dB improvements. Therefore, the overlay of configurations in Figure 9 represents a system with a high frequency reuse and at the same time an acceptable \bar{S}/\bar{I} value. This combination is totally beyond the reach of any mobile system and it can only be obtained in a fixed cellular system where the application of high-gain antennas for the subscribers is feasible. If the quality requirements in the system demand a

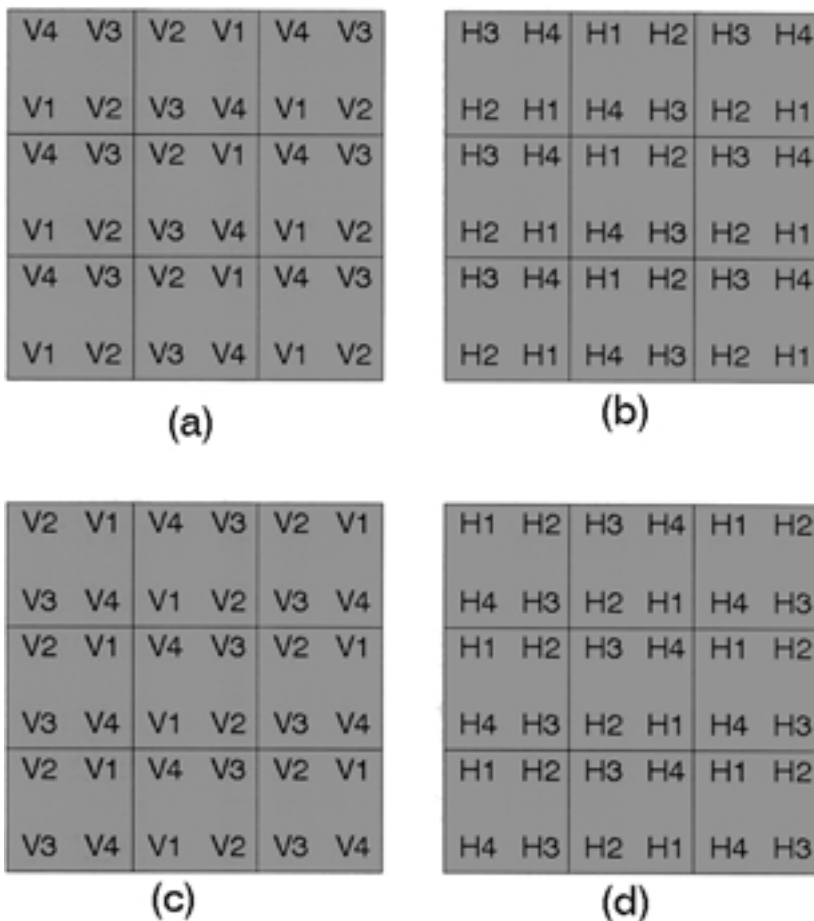


Fig. 9. Four Cellular architectures with frequency reuse of 1 and polarization interleaving. Each corner base station has a two-part designator: the letter shows the assigned polarization and the number represents the bandwidth segment.

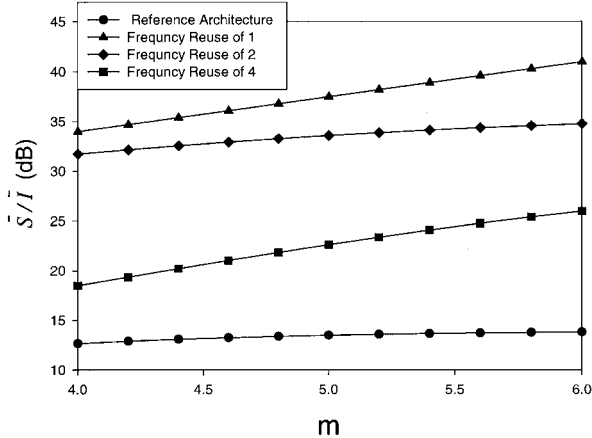


Fig. 10. \bar{S}/\bar{I} for individual cellular architectures of Figure 9 and their combination to form a new architecture with a higher frequency reuse. ($\sigma = 0$)

higher value for the \bar{S}/\bar{I} , the base station antennas with smaller angular span can be used, e.g., instead of four sector antennas in each base station, one can use 16 sector antennas. It should be mentioned that such a solution is not suitable to a mobile system when any increase in the number of base station sector antennas will increase the hand-off rate. On the other hand, for the fixed cellular systems hand-off is not an issue and at least theoretically the angular span of the base station antenna can be as small as the subscriber antenna.

Figure 11 shows the variation in \bar{S}/\bar{I} for the refer-

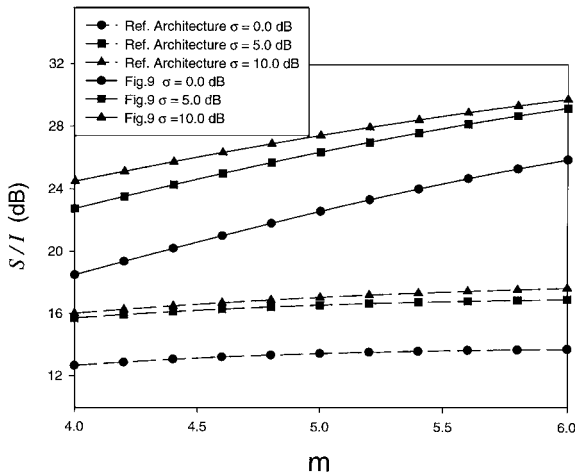


Fig. 11. Effect of the standard deviation of received signal on \bar{S}/\bar{I} for the combination of architectures in Figure 9 with a frequency reuse factor equal to 4.

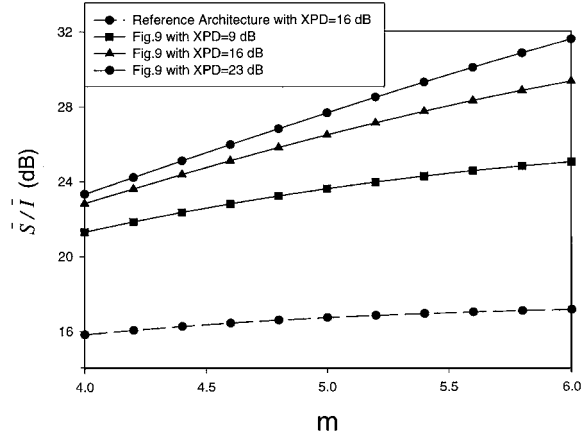


Fig. 12. Effect of the XPD on \bar{S}/\bar{I} for the combination of architectures in Figure 9 with frequency reuse of 4 and $\sigma = 5$ dB.

ence architecture and the proposed system in Figure 9 for different values of the standard deviation of the received signal. As it has been stated before, for a particular architecture, the values found for $\sigma = 0.0$ dB are the minimum values and as the variance is increased, a larger \bar{S}/\bar{I} is reached. However, this improvement has a saturation behavior and for example the difference between the values for $\sigma = 5.0$ dB and $\sigma = 10.0$ dB is small. In any case, the performance of the system with bandwidth segmentation and polarization interleaving always remains superior to that of the reference architecture.

Obviously, the effectiveness of polarization interleaving in our proposed system is a function of the depolarization by the medium. Therefore, it is instructive to investigate the influence of XPD on \bar{S}/\bar{I} . It has been stated in [3] that the most serious impairments were measured consistently in conifer tree stands where average XPD at 28.8 GHz was 9 dB for a foliage depth of 60 m. Figure 12 illustrates the variation of \bar{S}/\bar{I} for three values of XPD. Clearly, the proposed system maintains its superiority over a very wide range of XPD values.

IV. OUTAGE PROBABILITY FOR CELLULAR LMDS SYSTEMS

In previous sections, we only dealt with \bar{S}/\bar{I} . Over a fading channel, however, average values can be misleading and a better assessment of SIR is possible by calculating outage or finding the CDF of SIR. That is, the probability of SIR being smaller than certain threshold value.

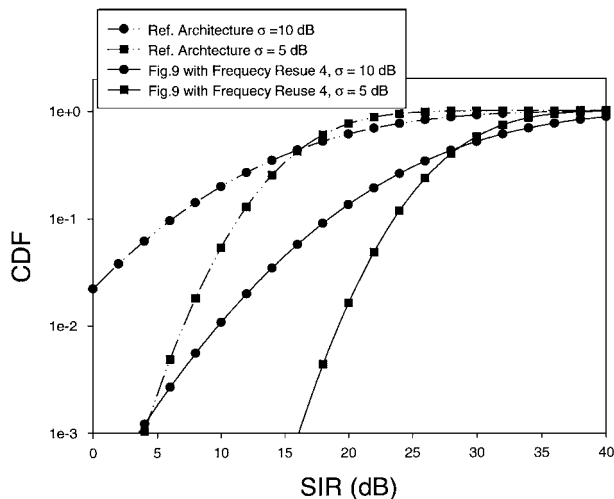
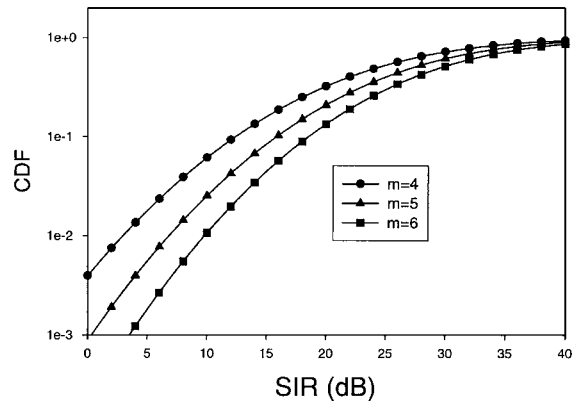


Fig. 13. CDF of SIR for Reference architecture and for combination of architectures in Figure 9 with frequency reuse of 4 and for $m = 6$.

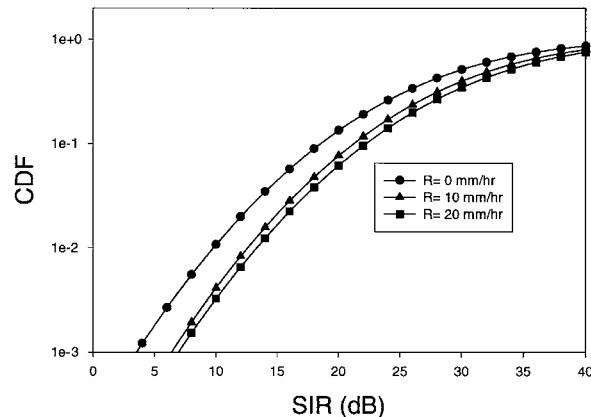
In this paper, CDF of SIR is found based on numerically computing equation (9) and finding the statistics of the total interference via Schwartz-Yeh method.

Figure 13 shows the CDF for SIR for the worst case point and for two different cellular configurations. Again, the superior performance of the architectures in Figure 9 is clear. For example, for a CDF = 0.01, the optimal configurations of Figure 9 promises at least 10 dB improvement, for the range of standard deviation between 5 dB to 10 dB, when compared to the reference architecture with the same capacity.

The final simulation results of this paper are shown in Figure 14 which shows the effect of medium attenuation on the SIR. As it can be predicted, Figure 14(a) shows that cellular systems working in a lossy medium are less susceptible to interference. This is due to the fact that as the medium becomes more attenuative, the contribution of the far interferer (Figure 3) diminishes. However, this is not true for the near interferers. Distance from the *worst point* to the desired base station is equal to the distance from this point to the near interferers and therefore any change in the attenuation of the medium would not change the contribution of these interference sources to the total SIR. This can be seen clearly in Figure 14(b) where the relation between SIR and rain attenuation is investigated. It can be seen that as the medium becomes more attenuative, i.e., at higher rain rates (R), CDF (SIR) tends to decrease and eventually saturates to a value set only by the near interferers. This is a very important observation because it shows during rainfall,



(a)



(b)

Fig. 14. Effect of medium attenuation on the CDF of SIR (a) for different attenuative media and $\sigma = 10$ dB, $R = 0$ (b) for various rain rates and $m = 6$, $\sigma = 10$ dB.

signal level drops but system becomes less susceptible to interference. Therefore, cellular systems can generate a higher level of interference to compensate the effect of power loss and maintain the initial service quality provided to the subscribers.

V. CONCLUSIONS

The results presented in this paper clearly demonstrate that although co-channel interference is a fundamental issue in fixed cellular systems but due to utilization of high-gain antennas, it is possible to have signif-

icantly higher capacities by reusing the available bandwidth several times.

The case study that we chose for our simulations is for line-of-sight and nearly line-of-sight LMDS architecture. In this regard, the related propagation issues in millimeter-wave frequencies like rain and foliage depolarization and attenuation are reviewed and it is claimed that depolarization by foliage is an important obstacle in reusing the bandwidth twice for each sector antenna. Following this argument we analyze \bar{S}/\bar{I} to show that a simple polarization interleaving, as a remedy for increasing the \bar{S}/\bar{I} , is not effective enough. We show that further improvement in \bar{S}/\bar{I} is possible by actually segmenting the available bandwidth. Using polarization interleaving and assigning these bandwidth segments to base stations in an intelligent manner shows around an order of magnitude improvement in \bar{S}/\bar{I} .

Analysis of *CDF (SIR)* confirms the above conclusions. Also, we show that during a rainfall or when the medium is subject to a high foliage attenuation, the main contribution of the interference is from near interference sources.

ACKNOWLEDGMENT

This research has been supported by National Science Foundation Grant Number CCR-9902846, Pennsylvania Ben Franklin Partnership Program and the Penn State University CICTR program.

REFERENCES

1. E. J. Voilette, R. H. Espeland, R. O. DeBolt, F. Schwering, "Millimeter-wave propagation at street level in an urban environment," *IEEE Trans. on Geoscience and Remote Sensing*, Vol. 26, No. 3, pp. 368–380, May 1988.
2. F. K. Schwering, E. J. Voilette, R. H. Espeland, "Millimeter-wave propagation in vegetation: experiments and theory," *IEEE Trans. on Geoscience and Remote Sensing*, Vol. 26, No. 3, pp. 355–367, May 1988.
3. P. Papazian, G. A. Hufford, R. J. Achatz, R. Hoffman, "Study of the local multipoint distribution service radio channel," *IEEE Trans. on Broadcasting*, Vol. 43, No. 2, pp. 175–184, June 1997.
4. R. A. Dalke, G. A. Hufford, R. L. Ketchum, "Radio consideration for local multipoint distribution systems," *NTIA Report 96-331*, Aug. 1996.
5. S. Martin, W. Myers, D. Burt, "Medium range terrestrial propagation study at 28 GHz," *SPIE Proc. 3232*, Wireless Techniques and Systems: Millimeter-wave and optical, pp. 33–43, Nov. 1997.
6. S. Y. Siedel, H. W. Arnold, "Propagation measurement at 28 GHz to investigate the performance of local multipoint distribution service," *Proc. IEEE Globcom 95*, Vol. 1, pp. 754–757, Nov. 1995.
7. D. C. Cox, "Co-channel interference considerations in frequency

reuse small-coverage-area radio systems," *IEEE Trans. on Communications*, Vol. 30, No. 1, pp. 135–142, Jan. 1982.

8. P. A. Gray, "A broadband wireless access system at 28 GHz," *Proc. IEEE Wireless Comm. Conf. 97*, pp. 1–7, Aug. 1997.
9. P. A. Gray, "Optimal hub deployment for 28 GHz LMDS system," *Proc. IEEE Wireless Comm. Conf. 97*, pp. 18–22, Aug. 1997.
10. S. C. Schwartz and Y. Yeh, "On the distribution function and moments of power sums with lognormal components," *BSTJ*, Vol. 61, No. 7, pp. 1441–1462, Sept. 1982.
11. Y. Yeh, J. Wilson, and S. C. Schwartz, "Outage probability in mobile telephony with directive antennas and macrodiversity," *IEEE JSAC*, Vol., No. 7, pp. 1441–1462, Sept. 1982.
12. N. C. Beaulieu, A. A. Abu-Dayya, P. J. McLane, "Estimating the distribution of a sum of independent lognormal random variables," *IEEE Trans. on Comm.*, Vol. 43, No. 12, pp. 286–2873, Dec. 1995.
13. R. C. Bernhardt, "Macroscopic diversity in frequency reuse radio systems," *IEEE JSAC*, Vol. 5, No. 5, pp. 862–870, June 1987.
14. R. C. Bernhardt, "RF performance of macroscopic diversity in universal digital portable radio communication: signal strength considerations," *Proc. IEEE Globecom' 85*, Vol. 2, pp. 1002–1007, Dec. 1985.
15. P. S. Henry, B. S. Glance, "A new approach to high-capacity digital mobile radio," *BSTJ*, Vol. 60, No. 8, pp. 1891–1904, Oct. 1981.
16. C. H. Hendrix, G. Kulon, C. S. Anderson, and M. A. Heinze, "Multigigabit transmission through rain in a dual polarization frequency reuse system: an experimental study," *IEEE Trans. On Commu.*, Vol. 41, No. 12, pp. 1830–1837, Dec. 1993.
17. D. V. Rogers, L. J. Ippolito, F. Davarian, "System requirement for Ka-band earth-satellite propagation data," *Proc. of IEEE*, Vol. 85, No. 6, pp. 810–820, June 1997.
18. S. Farahvash, and M. Kavehrad, "A Statistical channel model for millimeter-waves propagation in LMDS applications," *Proceedings of IEEE PIMRC' 99*, JAPAN, September 1999.
19. J. G. Proakis, *Digital Communications*, Third Edition, McGraw Hill, New York, 1995.
20. W. C. Jakes, *Microwave Mobile Communications*, J. Wiley and Sons, New York, 1974.



Dr. Mohsen Kavehrad, FIEEE, is a Professor of Electrical Engineering at The Pennsylvania State University. He received his B.Sc. degree in Electronics from Tehran Polytechnic Institute, in 1973, the M.Sc. degree from Worcester Polytechnic Institute (WPI) in Massachusetts, USA, in 1975 and his Ph.D. degree from Polytechnic University (Formerly: Brooklyn Polytechnic Institute), Brooklyn, New York, in November 1977 in Electrical Engineering. He has several years of industrial experience, primarily with the Bell Laboratories where he worked as a Member of Technical Staff. In March 1989, he joined the Department of Electrical Engineering at University of Ottawa, as a Full Professor where he was at the same time the director of Broadband Communications Research Laboratory. He was also the

leader of Photonic Networks and Systems Thrust and a project leader in the Telecommunications Research Institute of Ontario (TRIO), a project leader in the Canadian Institute for Telecommunications Research (CITR) and the Director of Ottawa-Carleton Communications Center for Research (OCCCR). He visited, as an academic visitor, NTT Laboratories in Japan, in Summer 1991. He spent a six month sabbatical as an academic visitor at NORTEL, Ottawa, in 1996.

In January 1997, he joined the Department of Electrical Engineering, The Pennsylvania State University as W. L. Weiss Chair Professor of Electrical Engineering and the Director of Center for Information and Communications Technology Research (CICTR). During 1997–1998 he was also the CTO and a Vice President at TeleBeam Inc., State College, PA. He visited, as an academic visitor, Lucent Bell Labs., New Jersey, Summer 1999.

He is a consultant to industry. He is also on the Advisory Committee of the Department of Electrical Engineering at Worcester Polytechnic Institute (WPI) in Worcester, MASS.

He is a former Technical Editor for the IEEE Transactions on Communications, IEEE Communications Magazine and the IEEE Magazine of Lightwave Telecommunications Systems. Presently, he is on the Editorial Board of the International Journal of Wireless Information Networks. He has chaired, organized and been on the advisory committee for several international conferences and workshops. He has worked in the fields of: satellite communications, microwave radio communications, portable and mobile radio communications, atmospheric laser communications, fiber optic communications and optical fiber networks. His current research interests are in Broadband Wireless Communications & Networking and Optical Communications & Networking. He has published over 250 papers and book chapters and holds several issued patents in these areas. He has published over 250

papers and book chapters and holds several issued patents in these areas. He was elected a Fellow of the IEEE in January 1992 for his contributions to Digital Wireless Communications and Optical Systems and Networks. Also, in 1992, he was elected as an IEEE Communications Society "Distinguished Speaker." He received 3 Exceptional Technical Contributions awards while working at Bell Laboratories, the 1991 TRIO Feedback award for his patent on a "Passive Optical Interconnect" and 5 best paper awards plus a Canada NSERC Ph.D. Thesis Prize, jointly with his graduate students at University of Ottawa.



Shayan Farahvash received his Ph.D. in electrical engineering from Penn State University in Dec. 1999. From 1996 to 1997 he worked as a research associate in Ottawa University working on fiber gratings. His research interests include fixed wireless communication systems, guided wave gratings and RF synthesizers. Presently, he is a senior member of technical staff in Hughes network systems, Germantown, Maryland.